Hindawi
Journal of Chemistry
Volume 2023, Article ID 9876157, 1 page
https://doi.org/10.1155/2023/9876157

Retraction

Retracted: Electrochemical Seismic Design and Artificial Intelligence System Modeling of High-Rise Steel Structure Buildings

Journal of Chemistry

Received 15 August 2023; Accepted 15 August 2023; Published 16 August 2023

This article has been retracted by Hindawi following an investigation undertaken by the publisher [1]. This investigation has uncovered evidence of one or more of the following indicators of systematic manipulation of the publication process:

(1) Discrepancies in scope
(2) Discrepancies in the description of the research reported
(3) Discrepancies between the availability of data and the research described
(4) Inappropriate citations
(5) Incoherent, meaningless and/or irrelevant content included in the article
(6) Peer-review manipulation

The presence of these indicators undermines our confidence in the integrity of the article's content and we cannot, therefore, vouch for its reliability. Please note that this notice is intended solely to alert readers that the content of this article is unreliable. We have not investigated whether authors were aware of or involved in the systematic manipulation of the publication process.

Wiley and Hindawi regrets that the usual quality checks did not identify these issues before publication and have since put additional measures in place to safeguard research integrity.

We wish to credit our own Research Integrity and Research Publishing teams and anonymous and named external researchers and research integrity experts for contributing to this investigation.

The corresponding author, as the representative of all authors, has been given the opportunity to register their agreement or disagreement to this retraction. We have kept a record of any response received.

References

[1] W. Xia, "Electrochemical Seismic Design and Artificial Intelligence System Modeling of High-Rise Steel Structure Buildings," *Journal of Chemistry*, vol. 2022, Article ID 8693110, 8 pages, 2022.

Hindawi
Journal of Chemistry
Volume 2022, Article ID 8693110, 8 pages
https://doi.org/10.1155/2022/8693110

Research Article

Electrochemical Seismic Design and Artificial Intelligence System Modeling of High-Rise Steel Structure Buildings

Wenjie Xia

Jinan Engineering Polytechnic, Jinan City, Shandong Province 250000, China

Correspondence should be addressed to Wenjie Xia; 20162103771@mails.imnu.edu.cn

Received 24 April 2022; Revised 17 May 2022; Accepted 26 May 2022; Published 13 June 2022

Academic Editor: Aruna K K

This study aims to improve the mechanical earthquake-resistance ability of high-rise buildings' steel structures so that their safety performance is improved and their service life is prolonged. The simulation experiments on the response of the staggered truss steel structure are conducted in high-rise buildings to earthquake energy waves. First, MATLAB is used to build an experimental platform for earthquake-resistance evaluation of high-rise residential buildings. Through the high-rise building model training, it is found that the model meets the needs of the study. Second, the earthquake-resistance performance parameters, deformation recovery capacity, and dynamic response speed of the staggered truss steel structure are simulated and tested. After earthquake energy waves with different intensities are posed on the high-rise building model, the performance parameters of the staggered truss structure are tested, and the changes in the parameters of the structure are analyzed. Finally, the earthquake-resistance performance and post-earthquake recovery ability of the staggered truss structure are tested through comparative analysis. The results show that the interlayer displacement fluctuation of the staggered truss steel structure is the smallest, and the earthquake resistance performance is better than others under the energy waves of all kinds of earthquakes. Although its earthquake-resistance ability decreases with the duration of earthquakes, the reduction speed is slow. When the quake lasts 12 s, the resistance of the staggered truss structure is still greater than 2500 MPa. This study provides a reference for the staggered truss structure of high-rise buildings.

1. Introduction

With the improvement of China's economic level, urbanization is also accelerating rapidly, and residential areas in the city are becoming increasingly insufficient. In response to solving the problem, some real estate developers tend to build high-rise buildings, which can save development costs and also attract residents. As China's geographical location is in the earthquake zone, many cities are near the earthquake zone. This brings challenges to the development of high-rise buildings. Therefore, the mechanical earthquake resistance of steel structures of high-rise buildings attracts more and more attention.

Steel materials are widely used in high-rise buildings because of their lightweight, high strength and hardness, good environmental protection, and earthquake resistance [1]. The earthquake-resistance ability, deformation performance, and dynamic response of the steel structure are analyzed. When the earthquake occurs, the load bearing of the steel structure is the response of external load and the strong inertia based on its mass [2]. The steel structure with a good deformation ability and excellent elasticity can protect the main body of the building because it can dissipate the energy generated by the earthquake.

With the optimization and development of architectural design, the steel structure applied in high-rise buildings is also developed [3]. A mathematical model of the structure of high-rise buildings is established, and the numerical simulation of each structural material under the action of earthquake energy waves is analyzed. The earthquake-resistance performance of the structure of high-rise residential buildings is evaluated from vertex displacement, interlayer preparation, and base shear force. Based on the experimental results, the static elastic-plastic analysis of the structure is made using finite element analysis software, and the earthquake-resistance performance of the structure under different intensities is calculated. The results show that high-rise buildings' staggered truss steel structure has good earthquake resistance, deformation recovery, and rapid-response ability. This study provides a reference for studying the steel structure of high-rise buildings.

2. Mechanical Earthquake-Resistance Ability of the Steel Structure

This research on earthquake resistance of high-rise buildings responds to the influence of natural disasters such as earthquakes. The way to improve high-rise buildings' earthquake-resistance ability is to design an earthquake-resistant structure as the main body of the building. Generally, architects select the steel structure with good performance in constructing high-rise buildings. The steel structure has a good bearing capacity and deformation ability, reducing damage and avoiding casualties and economic loss in natural disasters.

2.1. Staggered Truss Steel Structure. In high-rise buildings, the staggered truss steel structure mainly takes the building panel, truss structure, and load-bearing column as the basis [4]. The unilateral truss is arranged along the vertical direction of the interlayer, and the adjacent truss is staggered [5]. One side is connected to the top, and the other is connected to the bottom of the adjacent truss. The two ends of the truss are supported on the bearing column of the main building [6].

Such a unique structure can give the staggered truss steel structure a good deformation performance. The building staircase load in the vertical direction is transmitted and concentrated on bearing columns [7], avoiding deformation [8, 9]. The horizontal load on the building is transmitted to the floor through the staggered truss mechanism. Since the staggered truss mechanism in the interlayer provides sufficient lateral stiffness for the building body, there will be no excessive displacement in the horizontal direction under the action of horizontal load. The staggered truss steel structure is shown in Figure 1.

The vertical load on the main body acts on the upper and lower chords of the staggered truss structure, which can concentrate the load to the nodes of the truss. The extreme load should be considered in the joint design of the staggered truss structure. In the calculation, it is supposed that the ends of diagonal web members and vertical members are hinged, and the upper and lower chord members are the continuous beams hinged with columns at the ends. The truss uses the tension monoclinic web member system to clarify the transmission direction of forces. There is no inclined rod between midspan nodes and its shear force is borne by a chord. The walkway should be placed at the part with small shear forces, and it can be located at the quarter-point to meet the needs of setting suites. Because there is no vertical bar between the fasting nodes, the chord cannot be regarded as a member only bearing axial force. When subjected to the transverse load, the chord will bend. The shear and bending moment of the chord shall be calculated and its bearing capacity shall be checked. However, under the action of vertical loads, the shear force on the chord in the middle node is zero, while the shear force on the chord in the other nodes is also very small and can be ignored, so the truss is simplified into a statically determined structure.

In the calculation, the end reaction can be calculated, and then, the section or node method can be used to calculate the truss. The structural lateral displacement curve shows the influence of high-order vibration modes based on the static elastoplasticity of the model and the structural uncoupled vibration theory, displacement response spectrum theory, and the transformation relationship between the multi- and single-degree-of-freedom system. From the elastic natural vibration period and corresponding vibration modes under each vibration mode, the equivalent and lateral displacement curves of the equivalent single degree of each vibration mode are obtained; the overall elastic lateral displacement is also obtained. According to the assumption, the lateral displacement curve under a certain performance level is determined.

2.2. Earthquake Resistance of High-Rise Buildings. The evaluation of the earthquake-resistance ability of high-rise residential buildings needs to establish the dynamic equilibrium equation of the multi-degree-of-freedom system of the original structural column under ground acceleration and calculate the equivalent mass of the equivalent single-degree-of-freedom system, the equivalent restoring force, and the equivalent damping. According to the calculated results, the calculation equation of base shear and displacement at the yield point of an equivalent single degree-of-freedom system is given. Finally, the spectral velocity and spectral displacement are calculated. The performance evaluation of the building's structural columns is realized by the superposition of the two [10, 11].

If the deformation vector of the earthquake-resistance response of a high-rise residential building is $|\Phi|$, the dynamic equilibrium equation of the multi-degree-of-freedom system of the original structure column under ground acceleration is as follows:

$$[M]|\ddot{x}| + [C]|\dot{x}| + [Q] = -[M][I]\ddot{x}_{\varepsilon}, \tag{1}$$

where $[M]$ and $[C]$ represent the mass and damping matrix of multi-degree of freedom, respectively, $|\ddot{x}|$ and $|\dot{x}|$ represent the relative acceleration and relative velocity vector, respectively, $[Q]$ represents the restoring force vector, $[I]$ represents the unit vector, and $\ddot{x}_{\varepsilon}$ represents the motion acceleration of structural columns relative to the ground.

According to equation (1), the equivalent damping of the building structure column can be calculated. The expression equation is as follows:

$$C^{\varepsilon} = |\Phi|^{\tau}[C]|\Phi|\frac{|\Phi|^{\tau}[M][I]}{|\Phi|^{\tau}[M]|\Phi|}, \tag{2}$$

(a) (b)

Figure 1: Staggered truss steel structure. (a) The staggered truss steel structure in reality; (b) a 3D model of the staggered truss steel structure.

where $|\Phi|^{\tau}$ is the deformation vector of the structure column in energy wave dissipation.

According to the pushover analysis of the multi-degree-of-freedom structure of the original structure column, the relationship between force and deformation of the equivalent single-degree-of-freedom system of the building structure column can be calculated. The relationship between the base shear force and displacement at the yield point is calculated by using the following formula:

$$x_y^{\varepsilon} = \frac{|\Phi|^{\tau}[M]|\Phi|}{|\Phi|^{\tau}[M]|I|x_{k,y}}, \quad (3)$$

where x_y represents the vertex displacement of the building structure column and x_k represents its base displacement.

The demand spectrum curve of the building structure column is established. The 5% damping elastic acceleration response spectrum of the building structure column transforms the relationship between spectral acceleration S_0 and the inherent period T of the building structure column to its acceleration-displacement response spectrum. The calculation equation of the displacement spectrum of the building structure column is as follows:

$$S_k = \frac{T^2}{4\pi^2} S_0. \quad (4)$$

Equation (4) can calculate the earthquake resistance of the structure column.

First, the earthquake-resistance ability index of the building structure column is calculated, including the strength index and ductility index of the vertical components and the horizontal lateral bearing ability of the vertical components. Then, the total horizontal lateral bearing ability of the building structure column is determined according to the condition of the lateral displacement and deformation of the residential floor. The strength index of the structure column is calculated by the vertical components of the residential floor. The ductility index is the contribution of each component to the earthquake resistance ability of the structural columns.

If the assessed high-rise residential buildings have different vertical components, their components should be calculated separately. The calculation is determined according to the vertical component with the slightest. The total horizontal lateral bearing ability to build structure columns is determined according to the lateral deformation degree of residential floors. If the ductility index of building structural columns is $F = 1.0$, the building structure is calculated according to the area of the residential building walls [12]. The calculation equation of the earthquake-resistance ability index of building structural columns is as follows:

$$I_n' = \frac{\tau_\omega (nA_\varepsilon + A_\omega)}{\omega \sum A_f}, \quad (5)$$

where ω represents the value of the gravity load per unit area of the building structure column, A_ε represents the area of the building structure column of the residential floor, A_ω represents the area of the whole wall of the floor after the window hole and door hole of the residential building are deducted, $\sum A_f$ represents the sum of the area of the calculation layer of the residential building and the structural column of the superstructure, n represents the ratio of the shear modulus of the high-rise residential concrete to the structural column, and τ_ω is the standard earthquake and shear strength value of the structural columns damaged along the residential ladder sections.

The earthquake-resistance ability of the structural column is evaluated according to the calculation results of the earthquake-resistance ability index of building structural columns [13], the cumulative damage model of structural columns [14], the total dissipated strain energy of the structural column system, and the damage index of the building structural columns [15].

The cumulative damage model of the structure columns is implemented according to the life curve (N-s relationship) and the Miner criterion. Low-cycle fatigue life N of a parameter of the building structure column is calculated at any j cycle. The equation of the cumulative damage model of the structure column is as follows:

$$D_f = \sum \frac{1}{2N}. \quad (6)$$

A low-cycle fatigue model of structural columns under constant cyclic loading is implemented. The equation is as follows:

$$u_m - u_y = \left(\dot{u}_m - u_y\left(\left(\dot{2}N_f\right)^2\right),\qquad (7)$$

where u_m and $\dot{u_m}$ represent the peak displacement of the building structure column under the constant amplitude cyclic load and the peak displacement of the building structure column under the constant amplitude monotonic load, respectively, and u_y represents the yield displacement of the building structure column. N_f represents the low-cycle fatigue life of the building structure column (or the number of load cycles of the building structure column).

The damage index of the building structure column is compared with specific values [16]. When the damage index is between 0 and 0.15, it indicates that the building structure column is slightly damaged, showing that the earthquake-resistance ability of the building structure is good. When the damage index of the building structure is between 0.15 and 0.30, it indicates that there is a medium degree of damage in the building structure. When the damage index of the building structure is more significant than 0.80, it suggests that the building structure has been seriously damaged. The main body of the building has the risk of collapsing at any time, and its earthquake resistance is worst [17].

According to the requirements of "two stages and three levels," the earthquake-resistance effect calculated under the "good use" level is combined with the corresponding constant and live load effect (wind load effect and vertical seismic effect are considered when necessary). The component strength and stability are checked according to the combined internal force, and static elastic-plastic analysis is carried out after the section value is adjusted to check whether the designed structure meets the "personal safety" and the deformation limit requirements under the performance level of "preventing collapse." If it does not meet the requirements, readjust the member section and repeat the above design process.

In the MATLAB 8.0 environment, a test platform to evaluate the earthquake-resistance ability of the structural column is built, and simulation experiments are carried out using SeismoStruct.

2.3. Earthquake-Resistance Ability of High-Rise Buildings with the Staggered Truss Structure. Through the test platform for evaluating the earthquake-resistance ability, the earthquake resistance ability of the staggered truss structure under energy waves is tested. The specific experimental process is shown in Figure 2.

Figure 2 shows that the earthquake-resistance ability of high-rise buildings with the staggered truss structure is studied. First, the staggered truss structure is added to the high-rise building model. Then, the changes in the material properties of the staggered truss structure and the changes in the interlayer displacement angle of the structural column are tested under energy waves with different intensities. Thus, the response performances of other structures under energy waves with different intensities are obtained, and the earthquake-resistance performance of each structure is obtained. Finally, the stable performance of each structure is achieved by testing the energy dissipation rate of the structural columns in high-rise buildings.

The experiment is to explore the influence of relevant components and structural parameters on the deformation capacity, energy dissipation capacity, and reasonable failure mechanism of the staggered truss structure under earthquakes. According to the experiment and example analysis, the earthquake-resistance performance of the staggered truss structure is evaluated, and the design suggestions are put forward. The dynamic characteristics of the staggered truss structure and its response in elastic and elastoplastic stages under different records and strengths are summarized, including the internal force and deformation state in the earthquake-resistance response and the formation and development sequence of plastic hinges. The parts where stress and plastic deformation exist determine the yield mechanism's mechanism weak links and possible damage of the structure.

3. Analysis of Experimental Results

3.1. Relationship between Shear Stress and Time Variation under Different Accelerations. The change curves of shear stress and time of the simulation model under different accelerations are shown in Figure 3.

Figure 3 shows that under different accelerations, the changing trend of the shear stress of the staggered truss steel structure is the same, and the waveform is similar. the time of shear stress in positive and negative directions is consistent. The relationships between shear stress and the staggered truss steel structure time under different accelerations are compared. The results show that the time nodes of the maximum shear stress of the staggered truss steel structure on energy waves are inconsistent. If they are more than 5 s, there will be a gradual declining trend after the appearance of the peak.

3.2. Displacement Angle of Different Earthquake Resistance Structures under External Force. The interstory displacement angle of the structural column is calculated by the elastic method of the wind load, or the ratio of the maximum horizontal displacement between the residential floors and their heights under energy waves. It is an important index to measure the earthquake-resistance ability of structural columns. Four different methods are used to analyze the interstory displacement angles of the building structure columns, and their results are compared. The experimental results are shown in Figures 4 and 5.

Figures 4 and 5 show that when there is a small earthquake, the interstory displacement of the building structure without steel structure is largest, indicating that the earthquake-resistance ability of the structure is worst; under a large earthquake, the inter-story displacement fluctuation of high-rise buildings with the truss steel structure is most significant, proving that the earthquake-resistance ability of

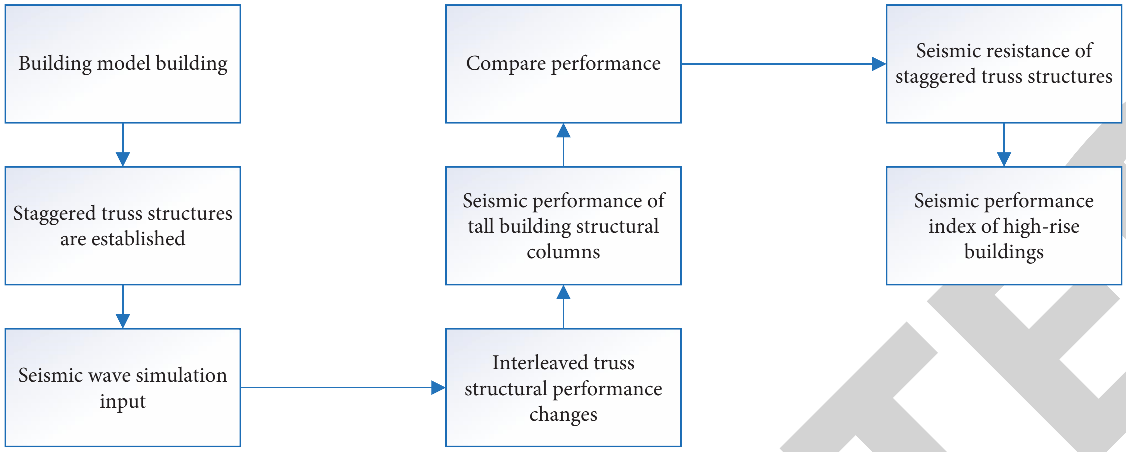

FIGURE 2: Experimental process of evaluating the earthquake-resistance ability of the structure column.

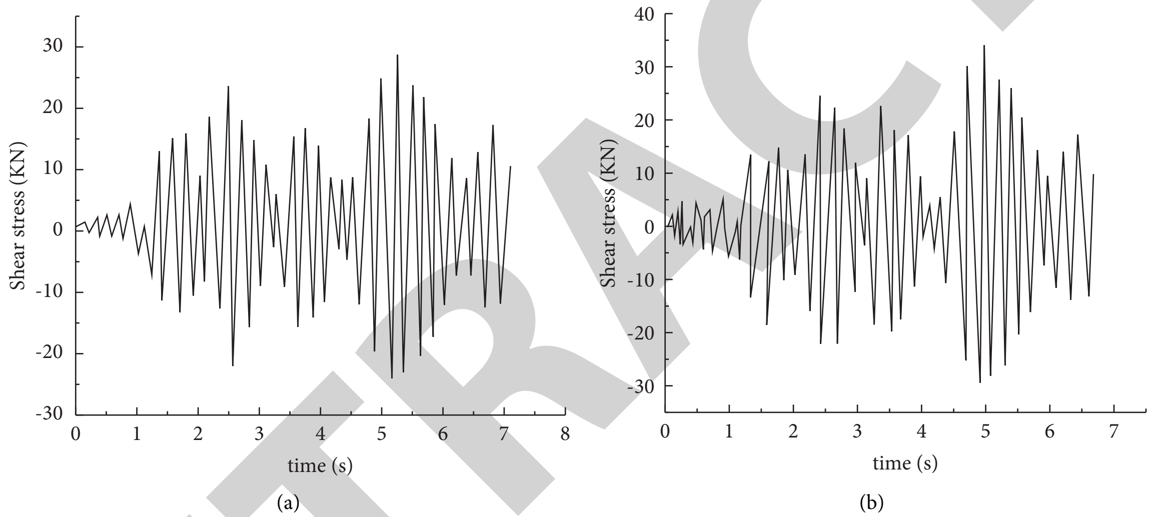

FIGURE 3: Relationship between shear stress and time under different accelerations. (a) The shear stress change at an acceleration of 50 gal; (b) the shear stress change at an acceleration of 100 gal.

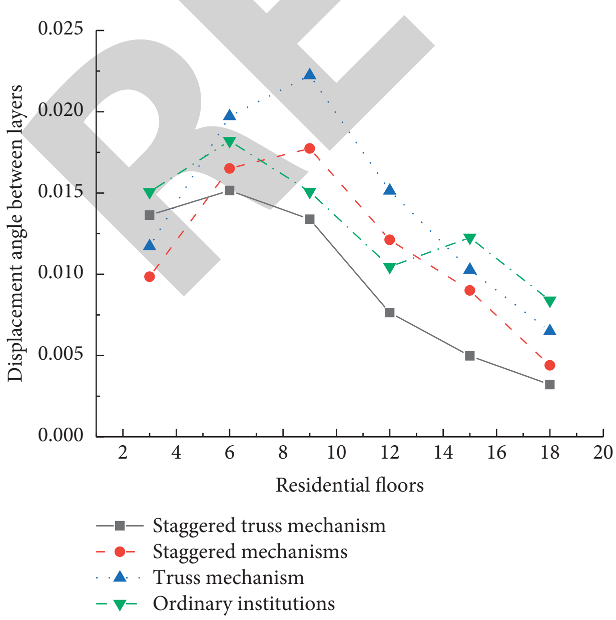

FIGURE 4: Interstory displacement angles of different floors under small earthquakes.

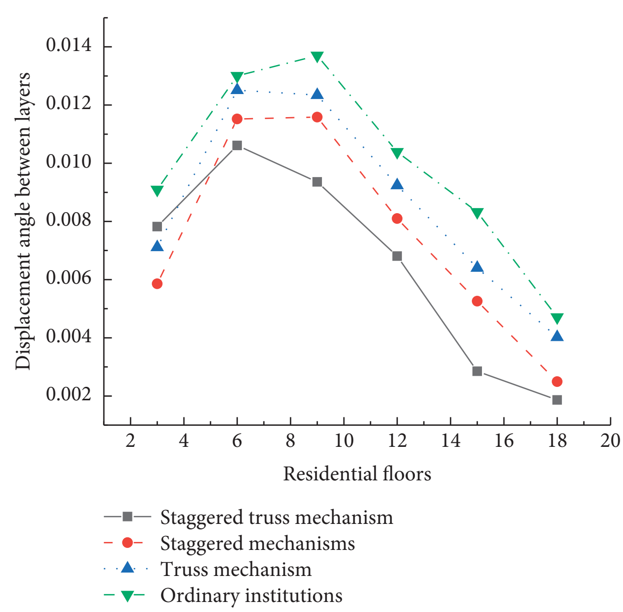

FIGURE 5: Interstory displacement angles of different floors under large earthquakes.

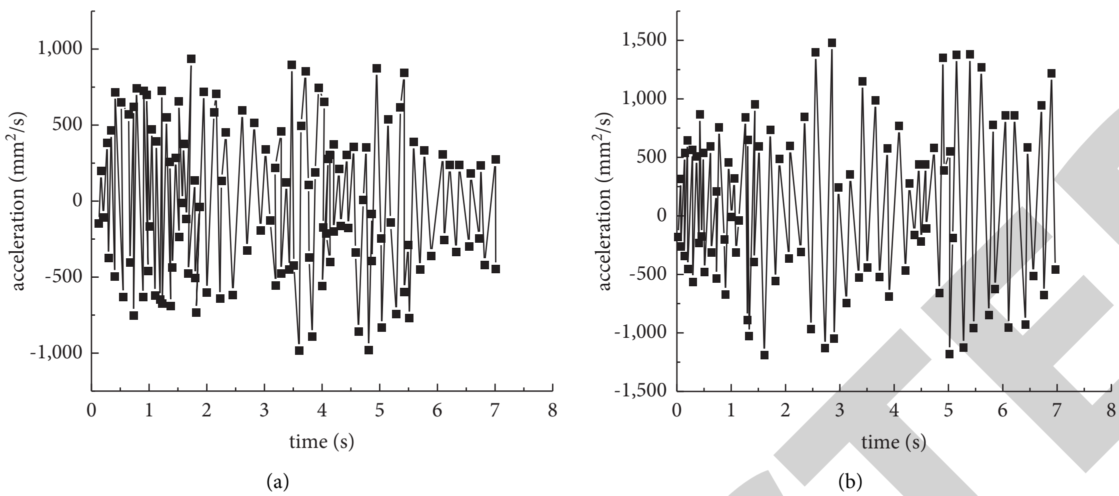

Figure 6: Acceleration-time curve of the staggered truss structure. (a) The time curve with a peak acceleration of 50 gal; (b) the time curve with a peak acceleration of 100 gal.

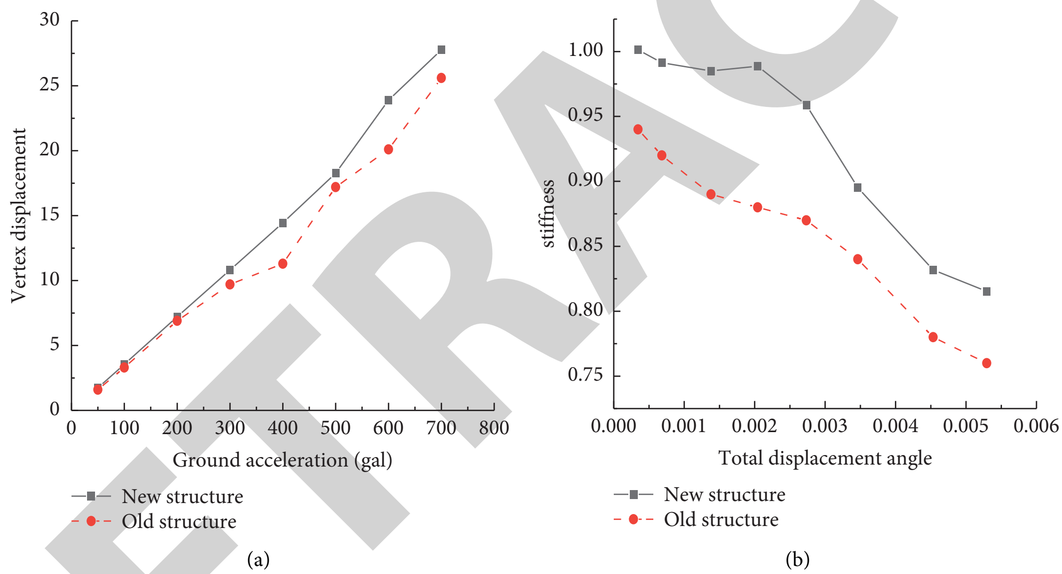

Figure 7: Relationship of total displacement, total displacement angle, and stiffness. (a) The relationship between ground acceleration and vertex displacement; (b) the relationship between total angular displacement and stiffness.

the structure is worst under large earthquakes; the interstory displacement of building structure columns with the staggered truss steel structure is stable under large earthquake and a small earthquake. However, its performance under moderate damage is not ideal; the interstory displacement of building structural columns is the smallest, and its performance is the best.

3.3. *Effect of Earthquake Waves on Acceleration.*

There are different accelerations under different earthquake waves, as shown in Figure 6.

The peak time of the top-level response acceleration is inconsistent with the peak time under the earthquake wave, and the former is lagged. This is because the natural vibration period of the structure is related to its earthquake wave period. The staggered truss structure has different conduction effects on different forces.

The relationship of total displacement, whole displacement angle, and stiffness in the staggered truss mechanism is shown in Figure 7.

Figure 7 shows that the structure is in an elastic state during the test, and the stiffness changes little. When the peak acceleration increases from 50 gal to 700 gal, the hysteresis curve of the structure is linear, and the energy consumption is less. The displacement response of the structure increases with the increase of the peak acceleration. When the peak acceleration is 600 gal, the structure first yields at the foot of the column. The slope of the hysteresis curve decreases and the stiffness degrades; the shape of the hysteresis curve shows that when the displacement is negative, the hysteresis curve deviates. This is because the

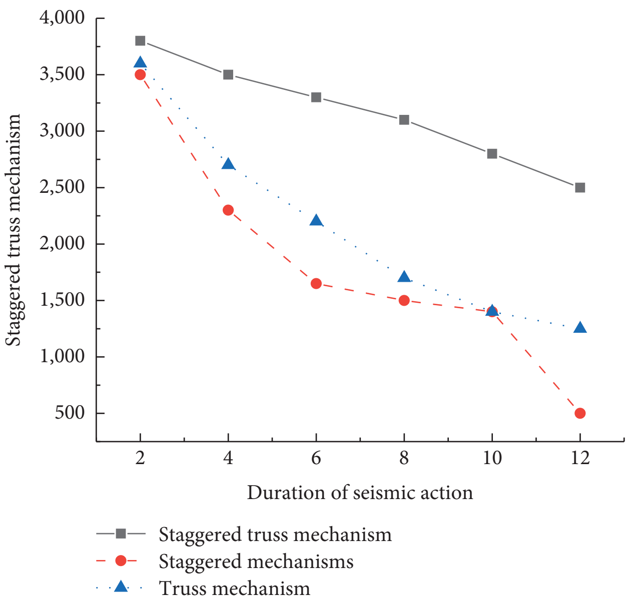

Figure 8: Stress changes of building columns with different structures.

elastic-plastic deformation caused by the round steel rod of the two loading beams on the top floor consumes part of the load, resulting in the displacement error of the actuator when it is pulled back. When the peak acceleration is 700 gal, the area of the hysteresis curve of the structure increases, indicating that the energy of the structure begins to dissipate and enters the elastic-plastic working stage.

3.4. Stress Changes of Building Structures. The stress of the structure column of high-rise residential buildings refers to the internal force generated by the interaction between the components of the building structure column when the building structure column is deformed under external forces (such as earthquakes, temperature changes, and humidity changes). The effect of the external force and the recovery of the structure column from deformation should be analyzed, and the effectiveness of the proposed method needs to be tested. Different methods are used to analyze the stress changes of building structural columns, and the results are compared. The comparison results are shown in Figure 8.

Figure 8 shows that the stress changes of the building structure column in the steel truss structure decreases the fastest with respect to the duration of earthquakes; when the earthquake lasts 12 s, the stress of the building structure column decreases less than 1000 MPa; when the duration of the earthquake is 8 s, the stress of the building structure column tends to be stable; when the earthquake lasts 12 s, the stress of the building structure column is reduced to less than 1500 MPa, and the resistance of the building structure column of the staggered steel structure is not ideal. In short, the stress changes of the building structure column of the staggered truss steel structure are reduced with the earthquake's duration, but the reduction rate is slow. When the earthquake duration reaches 12 s, the stress of the other two methods is less than 1500 MPa, and the stress of the building structure column is still maintained at 2500 MPa, which shows that the earthquake resistance of the structure column is best.

4. Conclusion

System modeling of the mechanical earthquake-resistance ability of high-rise buildings is studied. After a staggered truss mechanism is constructed, the earthquake-resistance ability of high-rise buildings is improved. Through the modeling and simulation based on MATLAB software, the simulation results show that the staggered truss mechanism has a strong load resistance and elastic performance along the direction of the truss, and its stiffness is not degraded under the action of the load. The staggered truss steel structure has excellent transferability for the stress generated by the load inside the building structure, which can significantly protect the building body. Under different earthquake waves, the staggered truss steel structure significantly affects high-rise buildings, which greatly improves the stability and bearing ability of high-rise building structural columns. However, there are some shortcomings that need to be improved. For example, only one type of the high-rise building model is selected in the simulation experiment, and the experiment results are not universal because there are few experimental samples. Besides, the staggered truss structure may influence the resistance ability of high-rise buildings, and the materials may also have a certain influence on the resistance of the staggered truss structures. A series of comparative experiments are needed to explore the influencing factors and the resistance of the structure of high-rise buildings.

Data Availability

The data used to support the findings of this study are available from the corresponding author upon request.

Conflicts of Interest

The authors declare that they have no conflicts of interest.

References

[1] B. Chen, W. Cheng, H. Ma, and Q. Yang, "Wind interference effects from one high-rise building and similar low-rise flat-roof buildings," *Journal of Structural Engineering*, vol. 147, no. 9, Article ID 04021138, 2021.

[2] S. Chapain and A. M. Aly, "Vibration attenuation in high-rise buildings to achieve system-level performance under multiple hazards," *Engineering Structures*, vol. 197, Article ID 109352, 2019.

[3] Y. M. Bazhenov, S. A. Murtazaev, D. S. Bataev, A. H. Alaskhanov, T. Murtazaeva, and M. Saydumov, "High-strength concretes based on anthropogenic raw materials for earthquake resistant high-rise construction," *Engineering Solid Mechanics*, vol. 9, no. 3, pp. 335–346, 2021.

[4] M. Sarcheshmehpour and H. E. Estekanchi, "Life cycle cost optimization of earthquake-resistant steel framed tube tall buildings," *Structures*, vol. 30, pp. 585–601, 2021.

[5] Z. Chen, B. Kim, and D. E. Lee, "Aerodynamic characteristics and lateral displacements of a set of two buildings in a linked tall building system," *Sensors*, vol. 21, no. 12, p. 4046, 2021.

[6] P. Fabris, "Strict seismic building codes credited with minimizing damage in Alaskan earthquake," *Building Design and Construction*, vol. 67, no. 6, pp. 76–79, 2018.

[7] H. Tang, "Recommended seismic performance requirements for building structures in Hong Kong," *Earthquakes and Structures*, vol. 15, no. 1, pp. 98–102, 2018.

[8] Y. Wen and J. Zheng, "Study on evaluating the seismic performance of building according to detail seismic condition," *Applied Mechanics and Materials*, vol. 4075, pp. 56–61, 2019.

[9] K. Nguyen, "Influence of building shape on wind-driven rain exposure in tall buildings," *Journal of Architectural Engineering*, vol. 27, no. 3, pp. 26–29, 2021.

[10] S. J. Suthar and R. S. Jangid, "Design of tuned liquid sloshing dampers using nonlinear constraint optimization for across-wind response control of benchmark tall building," *Structures*, vol. 33, no. 3, pp. 2675–2688, 2021.

[11] M. Arijit, "Amplification of seismic demands in inter-storey-isolated buildings subjected to near fault pulse type ground motions," *Soil Dynamics and Earthquake Engineering*, vol. 147, no. 5, pp. 86–89, 2021.

[12] F. Cluni, S. Fiorucci, V. Gusella, and M. Gioffre, "Estimation of the mechanical parameters for a reduced coupled flexural–torsional beam model of a tall building by a sub-structure approach," *Applied Sciences*, vol. 11, no. 10, p. 4655, 2021.

[13] Y. Qing, C. L. Wang, Z. Zhou, and B. Zeng, "Seismic responses of multistory buildings with self-centering buckling-restrained braces: influence of the pretension force," *Engineering Structures*, vol. 238, no. 2, Article ID 112249, 2021.

[14] R. Huang, P. Yan, and X. Yang, "Knowledge map visualization of technology hotspots and development trends in China's textile manufacturing industry," *IET Collaborative Intelligent Manufacturing*, vol. 3, no. 3, pp. 243–251, 2021.

[15] X. Liu, J. Liu, J. Chen, and F. Zhong, "Degradation of benzene, toluene, and xylene with high gaseous hourly space velocity by double dielectric barrier discharge combined with Mn3O4/activated carbon fibers," *Journal of Physics D: Applied Physics*, vol. 55, no. 12, Article ID 125206, 2022.

[16] M. Bradha, N. Balakrishnan, S. Suvi et al., "Experimental, computational analysis of butein and lanceoletin for natural dye-sensitized solar cells and stabilizing efficiency by IoT," *Environment, Development and Sustainability*, vol. 24, 2021.

[17] J. Dogra, S. Jain, A. Sharma, R. Kumar, and M. Sood, "Brain tumor detection from MR images employing fuzzy graph cut technique," *Recent Advances in Computer Science and Communications*, vol. 13, no. 3, pp. 362–369, 2020.